MMA Memo 253

Feasibility Study for a 12 m Submillimeter Antenna

Torben Andersen
European Southern Observatory
Karl-Schwarzschild-Str. 2
D-85748 Garching-bei-München
Germany

September 1997

EUROPEAN SOUTHERN OBSERVATORY

Organization Européenne pour des Recherches Astronomiques dans l'Hémisphère Austral
Europäische Organisation für astronomishe Forschung in der südlichen Hemisphäre

Large Southern Array

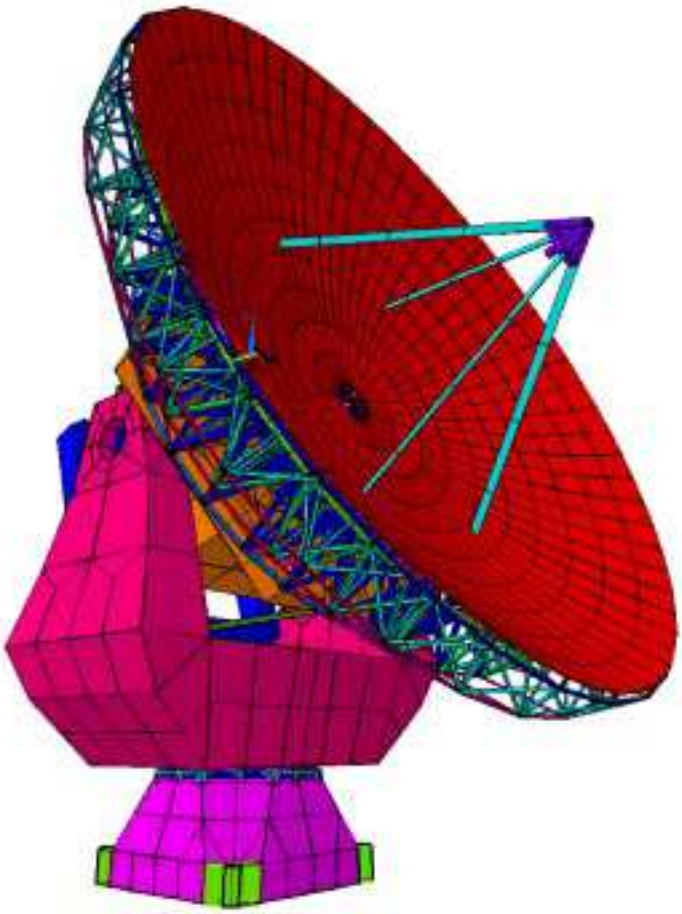

Feasibility Study for a

12 m Submillimeter Antenna

Torben Andersen
September 1997

European Southern Observatory
Karl-Schwarzschild-Str. 2
D-85748 Garching-bei-München
Germany

Ph. +49 89 320 06 0
Fax +49 89 89 320 2362

Abstract

A predesign is presented for a 12 m submillimeter telescope with a Carbon Fibre Reinforced Plastic dish structure. Calculations show that the telescope will passively fulfill requirements for a submillimeter telescope. Only calculations for representative cases have been carried out. A more detailed study will be needed to deliver the final proof that an antenna as proposed will fulfill all specifications

A differential pointing precision of 0.66" rms is required. This seems to be the most critical of all the specifications. Representative computations indicate that wind disturbances will cause pointing errors below 0.4" rms. Although there are also other error sources, this seems acceptable. More detailed computations are required for a final verification. To provide a larger safety margin, or alternatively a larger dish, it is attractive to develop a simple active optics system to correct for pointing errors caused by deflections in the steel structure below the elevation axis for frequencies up to 10-15 Hz. A possible implementation scheme is presented. A specification of 25 μm rms for the surface precision can be fulfilled.

A first transporter design is presented. Recommendations for project execution are given together with a tentative budget and time schedule.

Contents

1. Introduction 1
2. Antenna Design 2
  2.1 Optical Design 2
  2.2 Mechanical Design 3
    2.2.1 Dish 3
    2.2.2 Yoke 10
    2.2.3 Base 11
    2.2.4 Drives 11
  2.3 Foundation 12
  2.4 Control System 14
3. Antenna Performance 15
  3.1 Error Budget 15
  3.2 Optomechanical Performance 15
    3.2.1 Gravity Load 17
    3.2.2 Wind Load 19
    3.2.3 Thermal Load 20
    3.2.4 Eigenfrequencies 20
4. Prospects of Active Optics 22
  4.1 Active Optics 22
  4.2 Active Optics on Radio Telescopes 22
  4.3 Actions Proposed 24
5. Antenna Handling 26
  5.1 Transporter 26
  5.2 Assembly and Maintenance Halls 27
6. Project Execution 28
  6.1 Project Execution Principles 28
  6.2 Time Schedule 29
  6.3 Budget 30
7. Conclusions 32
8. Appendix A: Specifications 33
9. Appendix B: Locked Rotor Resonance Frequencies 36

1. Introduction

It is currently being discussed how a large array of submillimeter radio telescopes can best be built. An international committee has been formed to study different alternatives. The committee has the following members: John Lugten, NRAO, Peter Napier NRAO, David Wood, Caltech, Dietmar Plathner, IRAM, and Torben Andersen, ESO. Richard Hills, Cavendish Laboratory is participating as an observer. The committee is coordinating feasibility studies of various antenna types and sizes. The present study is one contribution to this work.

The aim of the present study was to assess the prospects for an economical 12 m submillimeter antenna. At the outset it was assumed that the antennas will be placed in northern Chile at the site Chajnantor near the town of San Pedro at an altitude of about 5025 m.

The antenna dish design proposed in the present study is based on the one of the IRAM 15 m Plateau de Bure radio telescopes. The author wishes to acknowledge highly important information received from Dietmar Plathner, IRAM.

The study was carried out at European Southern Observatory by the author of this report together with Franz Koch, ESO, Niels C. Jessen, Risø National Laboratory. Invaluable support was received from the Director of ESO, Professor Riccardo Giacconi, and Peter Shaver, ESO. Important information related to error budgets and costing was given by H. Kärcher, MAN.

2. Antenna Design

2.1 Optical Design

The antenna is of Cassegrain type. This has the advantage of low noise, little polarization and minimal blockage. The main parameters are shown in Table 1 and Figure 1 below.

Table 1. Main optical parameters.

	Primary	Secondary
Diameter	12 m	0.77 m
Radius of curvature	8.4 m	0.562 m
Eccentricity	1	1.092
Focal length	4.2 m	0.56 m
f-ratio	f/0.35	

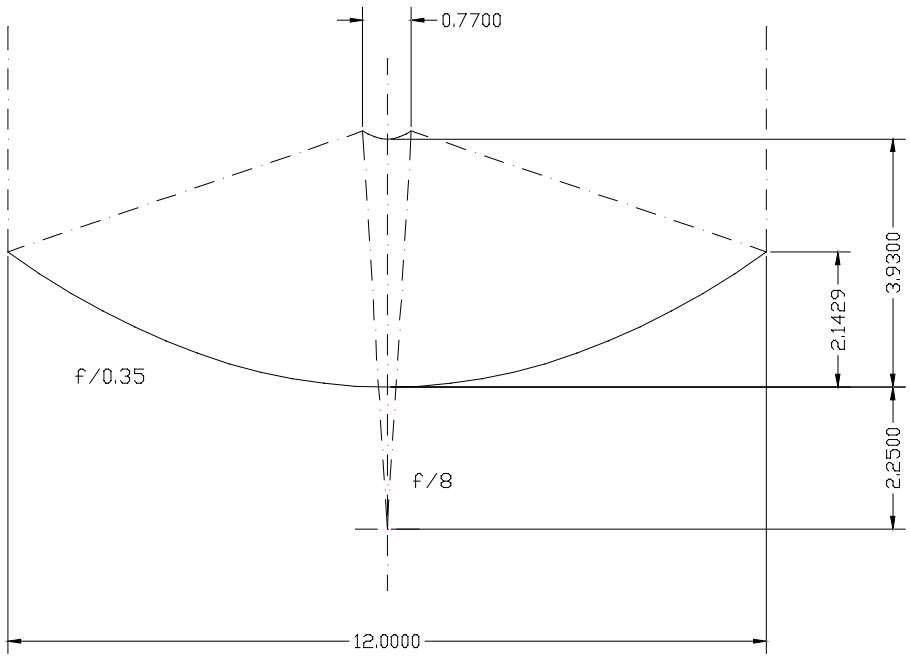

Figure 1. Optical Layout of antenna.

The exit f-ratio was chosen to be f/8. Such a value leads to a reasonable scale in the focal plane. The f-ratio may however easily be changed to f/10 or f/12 if receiver design should

call for a modification. No shaping has been assumed so far. In any case this will have only little importance for the results of this study. For the same reason, selection of amount of tapering has been left open at this moment.

From an optical point of view it is highly attractive to connect a tripod/quadrupod to the outer rim of the main reflector since this reduces obstruction of the light. However, for structural reasons it was not advantageous to do so. Hence the quadrupod does obstruct somewhat the light going from the main reflector to the subreflector. Obviously, the quadrupod legs should be as thin as possible. A value of about 20 mm has been chosen.

The 3 dB beam width at λ=1mm of the center peak of the antenna will be 17.4" without tapering, and 19.8" with 10 dB of tapering.

2.2 Mechanical Design

The proposed overall mechanical design is shown in Figure 2 and Figure 3. It will be shown in the following that this design fulfills the requirements. However, other designs may also be appropriate for the present purpose.

On the basis of discussions with potential users, the pointing range in elevation was chosen to be 15°-95°. With the present design, the lower limit is defined by structural interference between the lower dish structure and the yoke. The upper limit is set by the wish to be able to perform holography near zenith. The zenith range is ±270°.

In the following, individual design features are described in detail.

2.2.1 Dish

The dish has panels of an aluminum alloy and a backup structure (BUS) of carbon fiber reinforced plastic (CFRP).

The panels are of lightweighted aluminum. They are machined from solid blocks on a precise numerically controlled machine tool. The panels are fixed to node points of the BUS in the four corners. In addition, there is a fixation in the middle via a truss connecting the panel to a node point in the lower layer of the BUS. The panels are fixed to the BUS through studs that permit thermal expansion of the aluminum without introducing significant stresses into the BUS. The panels are adjustable through screws that are accessible from above. There are gaps between the panels to permit thermal expansion of the individual panels without squeezing the structure. The gaps between the panels will not be sealed. It is not foreseen to clad the BUS.

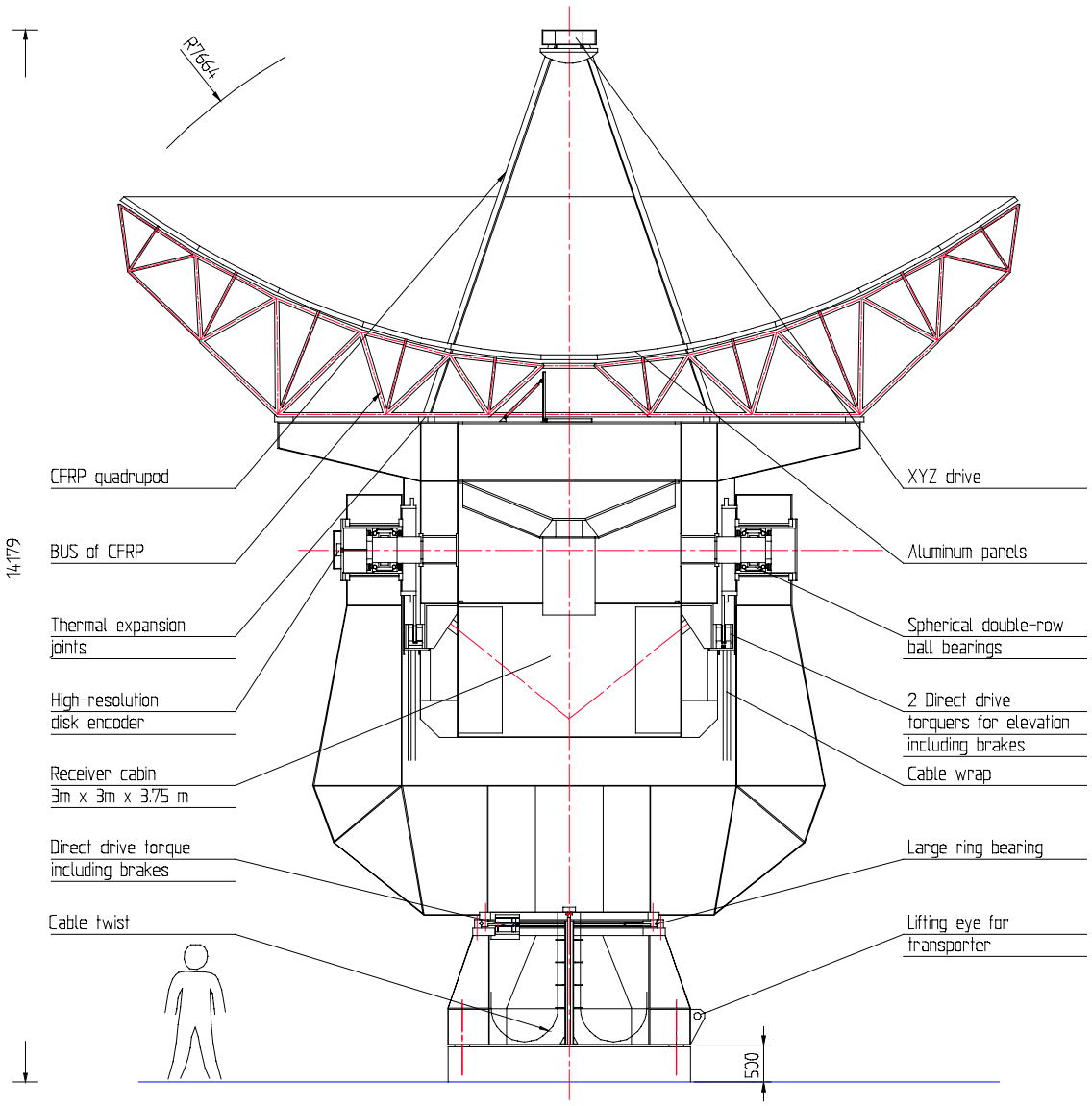

Figure 2. Proposed antenna design. Front view.

The panels can be aligned to a reasonable precision using a laser theodolite. Subsequently, the panels are precision adjusted on the basis of holographic measurements.

The surface roughness of the panels will be fine enough to reflect radio waves with wavelengths down to 0.35 mm. However, to permit observations of the Sun, there will be grooves machined into the panel surface with a depth of about 2 μm and with a geometry ensuring the major part of the solar incident energy to be reflected back to the sky, thereby protecting the subreflector and receiver against damage.

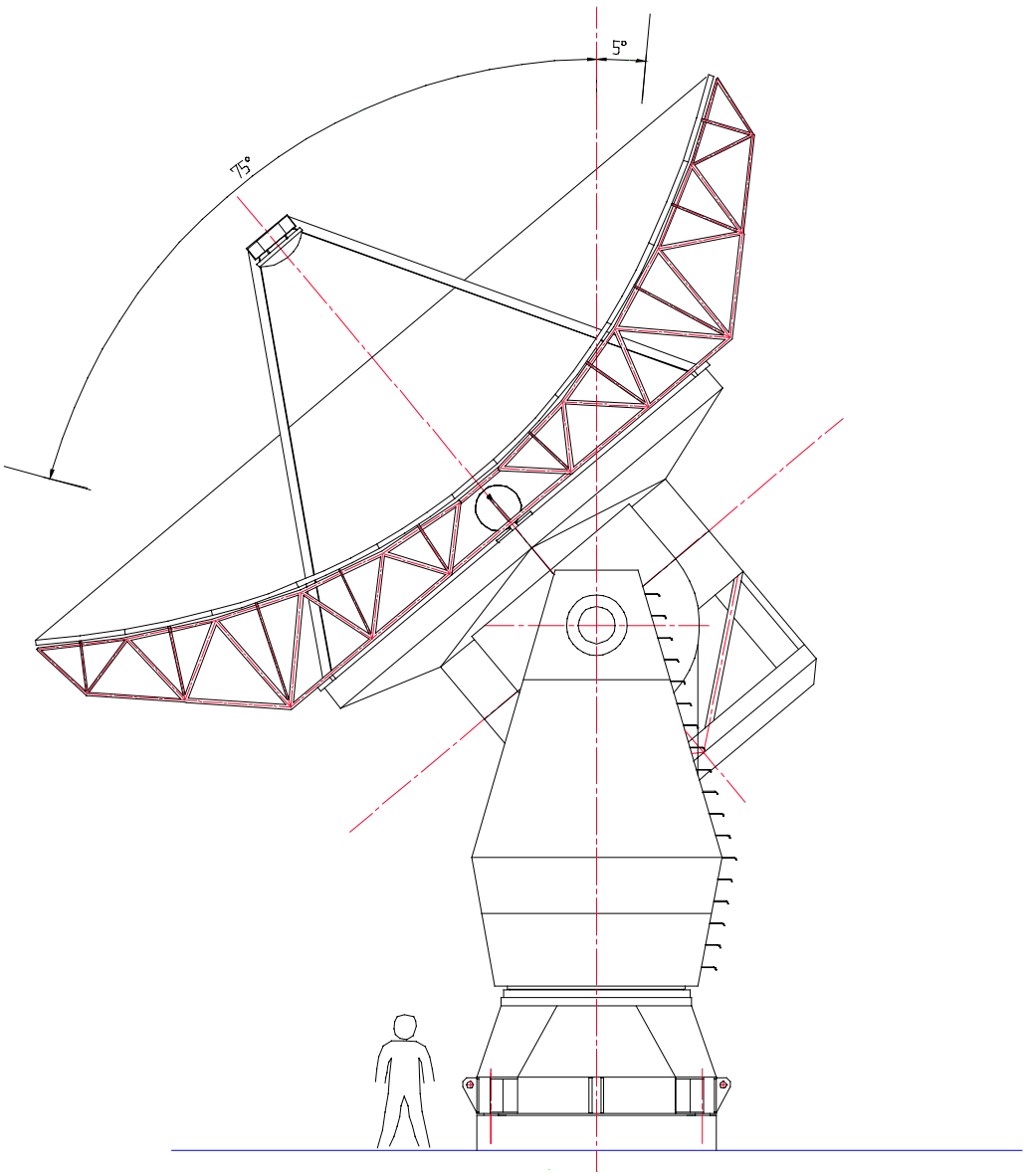

Figure 3. Proposed antenna design. Side view.

Heating of the panels for de-icing purposes is not foreseen. Snow and ice are rare on the site. Even if ice should build up, there seems to be only little risk that it would stay for long periods. The solar influx is significant so that the ice would melt during daytime.

The BUS is made of CFRP. Three dimensional drawings of the selected structure are shown in Figure 4 and Figure 5. At this moment, only a limited study of the dish alternatives has been carried out. Steel nodes are rather heavy and have thermal expansion problems. Hence, it would seem attractive to design a BUS with all or most node connections of CFRP. Since fabrication of the antennas would be done by "mass

production", it seems possible to use a 12 m jig for the epoxying of the BUS. The BUS could be epoxied together to one single part in the workshop and be transported to the site as an entity. In Chile, helicopter transport to San Pedro could be attractive. Fabricating the BUS'es over the same jig would ensure that all antennas have the same dimensions. Epoxying the trusses together would lead to a stiff and light structure. At the same time this approach would reduce the assembly work to be carried out in Chile.

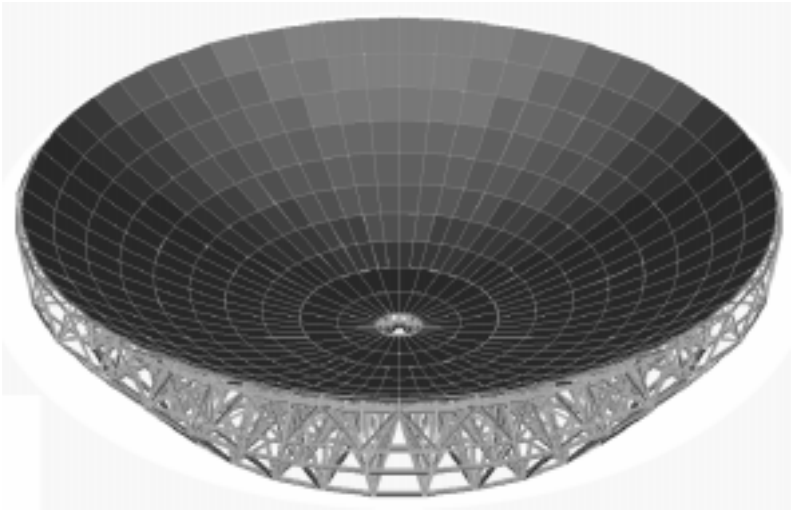

Figure 4. Back-Up Structure (BUS) with panels. Front view.

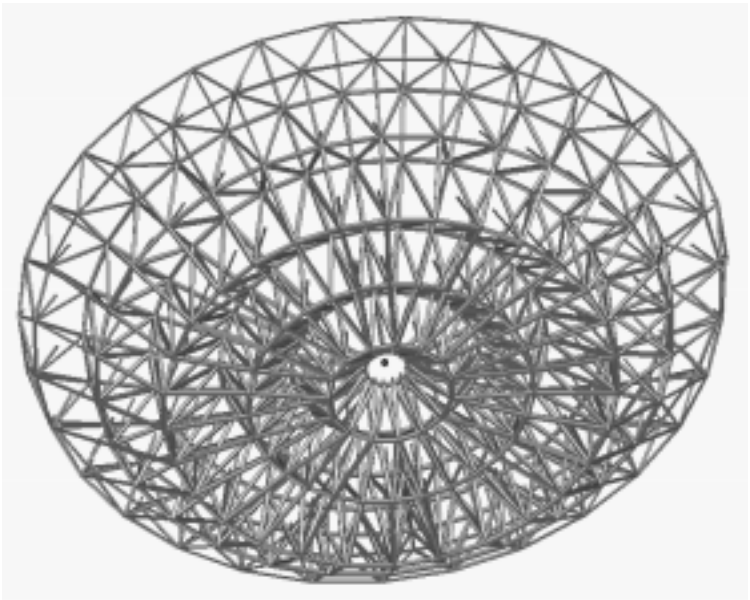

Figure 5. Back-Up Structure (BUS) without panels. Rear view.

Further studies are required to evaluate whether such an approach is indeed economically feasible. However, at the outset it seems to be the case and for the finite element calculations to be presented later it has been assumed that such a structure will be applied.

There are typically three types of structural designs in use for large antenna dishes:

a) Polar truss pattern with circular support
b) Polar truss pattern with central hub support
c) 120 degree truss pattern with circular support

The three different principles are shown in Figure 6.

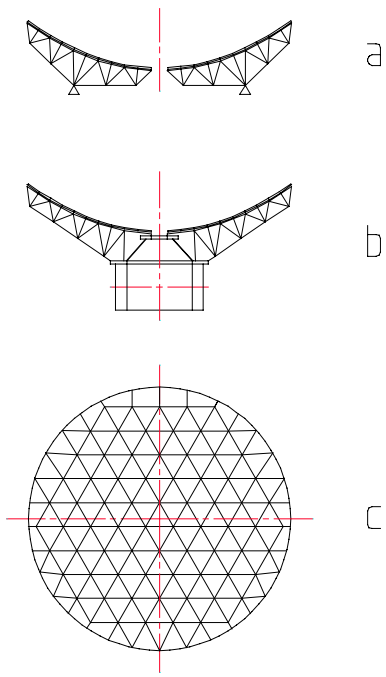

Figure 6. Different layouts of antenna dishes. Solution a) has a polar truss pattern with circular support, b) a polar truss pattern with central hub support, and c) a 120 degree truss pattern. a) and b) are side sections whereas c) is a top view of the truss geometry.

The *polar truss pattern with central hub support* (see Figure 6b)) has a dish that is supported from below at the central hub which typically is a large steel structure. This leads to considerable dish gravity deformations, since the dish is held in the center. The steel center structure has thermal expansion and this does not match well with BUS trusses of CFRP. The advantage of the design is that the dish attachment to a center piece inside the lower yoke is straightforward. Also, dish gravity deflections are well-behaved and a homologous design is achievable to a high degree. Such a design (see d)

of Figure 7) has been studied in some detail although finite element calculations have not yet been carried out for this solution.

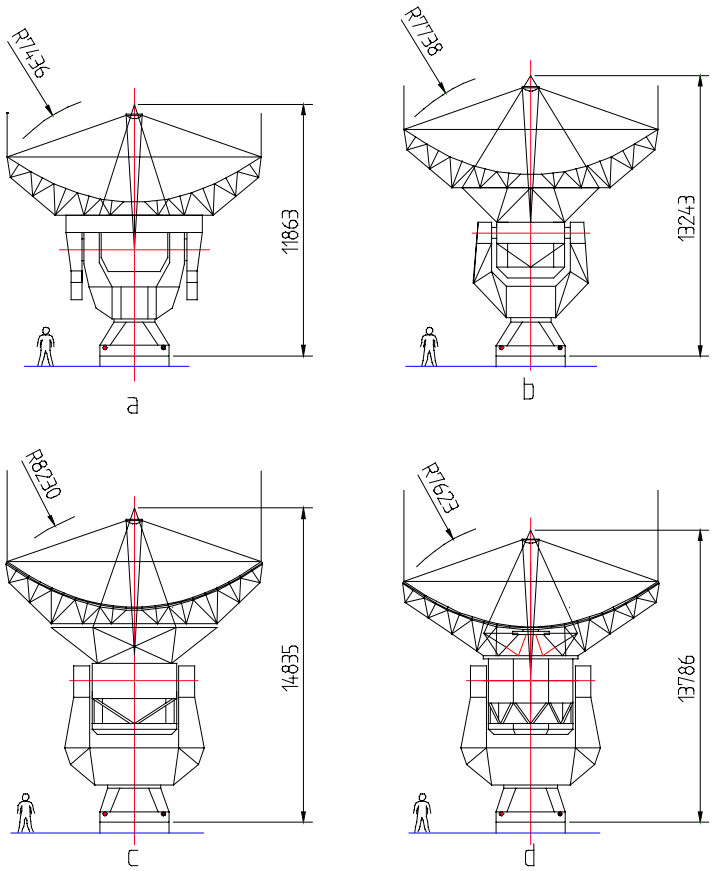

Figure 7. Some antenna design alternatives. Design a) has elevation shafts outside the yoke. This design is best for small receiver cabins. b) is a design with a yoke having a truss structure, and with a truss structure below the BUS. c) has a yoke of plate boxes and a truss structure connecting center section and BUS. d) shows a design with a central hub in the dish. The a) and b) designs have been drawn with smaller receiver cabins.

The *120 degree truss pattern* (c) of Figure 6) is highly attractive from a point of view of node point manufacturing. Node points usually tend to be costly. Due to the fact that many antennas must be produced, it may be of interest to study the 120 degree truss structure further. This has not been done so far.

The *polar truss pattern with circular support* has a backing steel structure that spreads out below the BUS of the dish and supports it at a diameter about half way out from the center. See a) of Figure 6. The advantage of the design is that axial gravity deflections of the dish can be kept smaller than for the central hub solution. The disadvantages are that dish gravity deflections do not resemble a paraboloid and that thermal expansion problems exist between the steel structure and the BUS of CFRP. This design seems

most attractive if one does not go for a pure homologous design but gives more emphasis on stiffness and small wind deflections. It is the design that has been chosen for the present proposal and that was shown in Figure 2 and Figure 3.

The thermal expansion of the steel structure below the BUS of CFRP is handled by special devices allowing radial movement between the steel and the CFRP structure. From the outset it was not clear whether these elements would be harmful to the performance of the antenna. To study this, a finite element model of the antenna dish was set up. Two different calculations were carried out. In the first one, the antenna was fixed to ground in all three translational degrees of freedom at the six interface points below the BUS. In the second one, radial freedom was introduced for the six support points between the BUS and ground. The lowest eigenfrequencies were 43 Hz and 36 Hz, respectively. Hence, it is concluded that the influence of the thermal expansion devices is not critical. The eigenmode corresponding to the latter situation is shown in Figure 8. This eigenmode is roughly equal to the internal eigenmode of the antenna dish when placed in the complete antenna.

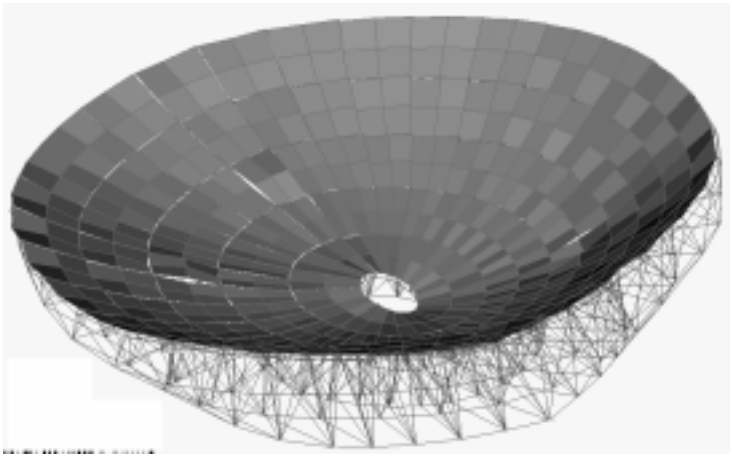

Figure 8. Eigenmode corresponding to the lowest eigenfrequency of the dish with thermal expansion devices included.

It would be possible to replace the steel structure spreading out below the BUS by a CFRP truss structure. Such a design is shown in c) of Figure 7. This design is lighter but such an antenna takes up more space sideways and cannot be packed as densely in an array as other antennas. Thus it was not studied further at this time.

The receiver cabin is quadratic in cross section and has access from below. It has a width of 3 m leaving adequate room for computer equipment. At the lower level of the receiver cabin (and outside it) there is a steel counterweight. It is supported by a simple truss structure and not by the cabin walls.

2.2.2 Yoke

The yoke is a conventional box structure of steel plates. It was found that the advantage of using CFRP is too small for this and other lower parts of the structure. The bearings in the yoke arms are spherical, double row bearings. Such bearings have the advantage that they do not require precise alignment or machining of the borings on the two sides of the yoke with respect to each other. Figure 9 shows a section through one of the arms of the yoke. In addition to the spherical bearing, the on-axis encoder of dish type can be seen to the left. Also, the direct-drive torque motor (without gears) is seen between the yoke arm and the center section. There are such motors on both arms thereby giving load symmetry. The motors have "normally closed" friction brakes included.

Near the elevation axis, between arm and center section, one or two cable wraps are placed.

In the lower part of the yoke, the yoke is connected to the base via a large ring bearing. See Figure 10. The bearing can be of cross roller type or "three ball row " type. The latter is stiffer. So far, it has been assumed that a cross roller bearing will be used since it has a lower cost. A more careful study of the performance will be needed.

At the interface between the base and the lower part of the yoke a direct-drive motor (without gears) is located. The motor has a "normally closed" friction brake. There is also a cable twist arrangement and an encoder.

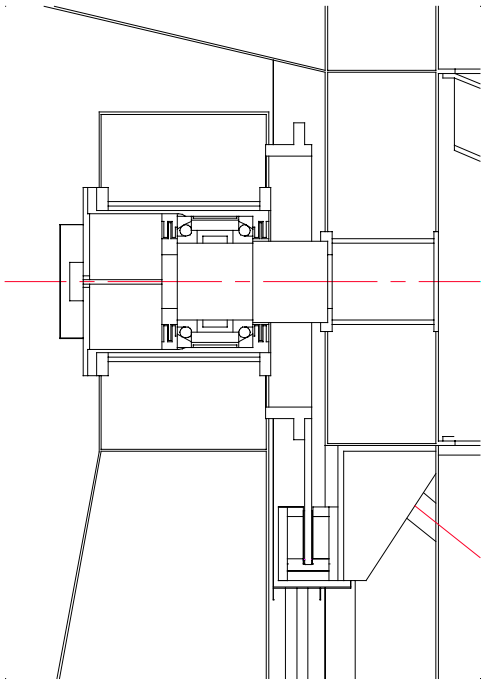

Figure 9. Section through one of the yoke arms. The spherical ball bearing and the direct drive torque motor can be seen.

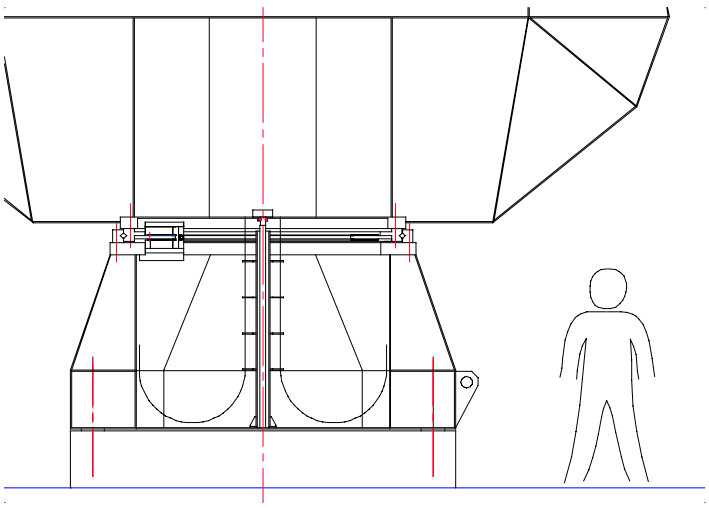

Figure 10. Section through the lower part of the yoke and the base.

2.2.3 Base

The base is shown in Figure 10. In addition to the interface to the yoke as described above, the base also interfaces to the foundation. It has been assumed that this takes place through hardened ball/cup arrangements located at the four corners of the base. The cups are embedded in the concrete foundation and the balls are fixed underneath the base. In addition there are four spindles to clamp the antenna to the foundation. The spindles are not motor driven. The maintenance team brings an electric wrench to attach the base to the foundation.

2.2.4 Drives

The main drives of the antenna will have direct-drive torque motors. This has the advantage of no internal friction and high stiffness as compared to using gears. In addition, torque motors are virtually maintenance free. Servos based on torque motors can be highly optimized since the motor and the load are directly coupled to the same axis.

For the elevation axis, two direct-drive torque motors are applied in parallel. The advantage is that only symmetric eigenmodes can be excited, for which reason a higher servo bandwidth can be obtained. The disadvantage is higher cost than for a solution with only one motor. The torque motor for the azimuth movement has been placed inside the large ring bearing. It could also be inverted and placed outside the bearing. This would have the advantage that the diameter becomes bigger and a more inexpensive motor can therefore be used. It also provides more easy access for maintenance. The main disadvantages are that it is less protected against dust and that it takes up space at the location of the transporter (see section 5.1).

For reasons of cost and simplicity, there will be no tachometer. The encoders have high resolution and a velocity signal can be deduced from the encoder signal. The encoders are of optically readable dish type, such as for instance Heidenhain RON905 with a smallest increment of less than 0.01".

The motor torques for different pointing angles for a wind velocity of 24 m/s are shown in Figure 11 and Figure 12.

The power amplifiers can be placed inside the fork together with other control electronics.

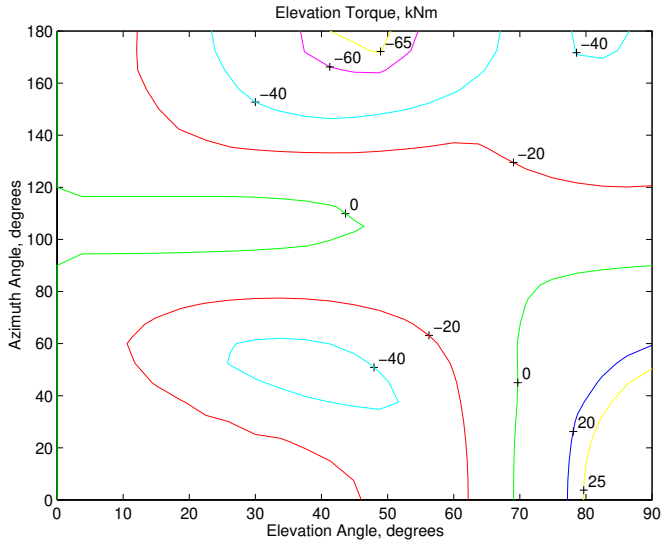

Figure 11. Total elevation motor torque for different pointing angles. Wind velocity 24 m/s.

2.3 Foundation

The radio telescopes will be movable between a number of observing stations. There could be about 60 telescopes and 240 observing stations.

At this time little information on soil quality is available. However, it is expected that the soil is similar to that on Hawaii and La Palma, i.e. loose volcanic material with an E-modulus of the order of 100 Mpa. This calls for a foundation with a large contact surface to spread out the load and to achieve a stiff support. In view of the large number of foundations, it seems important to avoid piling under the foundations. In case of doubt related to the soil quality, plastic tubes could be integrated into the foundations, thereby preparing for a later injection to stabilize the underground.

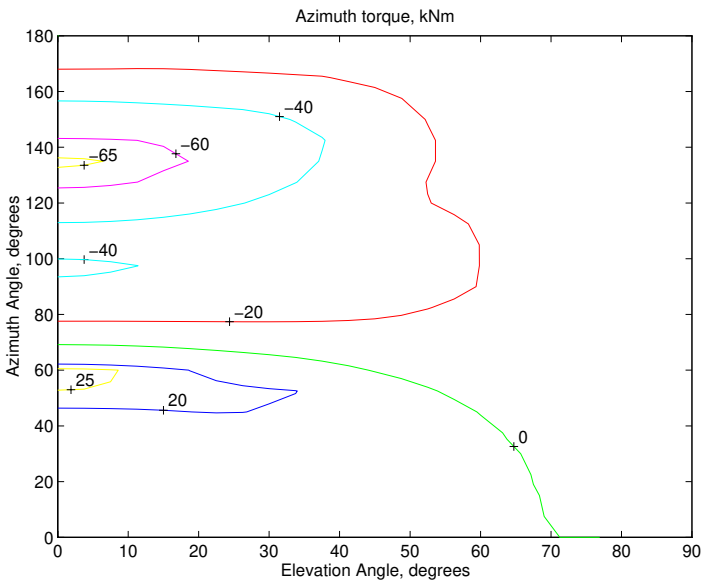

Figure 12. Azimuth motor torque for different pointing angles. Wind velocity 24 m/s.

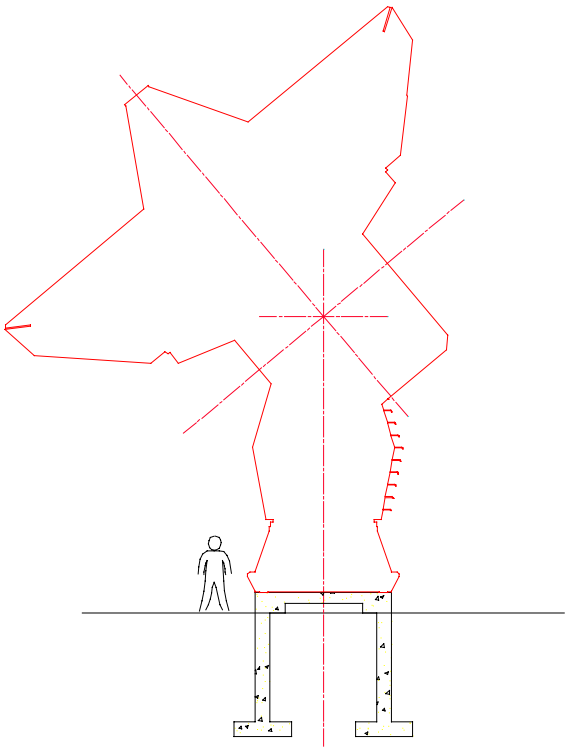

Figure 13. Tentative foundation design.

Another point is that the average temperature at the site is below 0°, which could conceivably result in permafrost. If this is indeed the case, it would be important to place the foundation sufficiently deep to avoid the annual melting of any water present under the foundation.

A tentative foundation design is shown in Figure 13. The upper surface of the foundation is lifted some 500 mm above ground to provide more easy access to the lifting eyes of the antenna. The antenna positioning cups described in section 2.2.3 will be cast into the concrete very precisely. The same (or identical) jigs will be used for all foundations.

2.4 Control System

The control system has not been studied in any detail at this time. It is anticipated that there will be no feasibility problems. There will be a distributed control system for the antenna array. Each antenna will be controlled from its own VME station, possibly running VxWorks, so that only power, a time bus, and a communication fiber link are required for antenna control. In addition other links are needed for receivers and their electronics.

There will be two main servos for elevation and azimuth and three smaller ones for movement of the subreflector to compensate for gravity deflections. The main servos are thought to have cascade controllers with current, velocity and position loops. The velocity signals are generated from the encoder readings. The current loop will be analog, whereas the velocity and position loops should be digital with a sampling period of not more than 1 ms.

There will be automatic control of the lid of the receiver cabin so that it is closed when the antenna is not in use. In addition, the brakes for the main axes will be operated automatically. Also, an overspeed monitor is needed.

3. Antenna Performance

In the following section the error budgets for the antenna are set up. Thereafter computations showing the performance level of the antenna are presented.

3.1 Error Budget

Due to the limited nature of this study, it is not possible to establish error budgets in great details. Table 2 presents the surface error budget for the complete telescope and Table 3 the differential pointing error budget. The surface error budget is a combination of effects at the main reflector and the subreflector. It can be conceived as 0.5 times the wavefront error of the waves going to the focus. The values for the subreflector include effects from its support structure and the adjustment mechanisms. The pointing error budget is concerned with pointing errors from an offset after nulling at a known target, and within the subsequent 30 minutes during tracking. For both error budgets, it is assumed that the error distribution is such that the errors can be combined by taking rss values.

Table 2. Surface error budget. All values are in μm.

Item	Error Type					
	Manufact.	Alignm.	Gravity	Temp.	Wind	Total
Panels	15	7	2	3	3	17
CFRP BUS	0	0	4	6	3	8
Steel struct.	0	0	4	4	3	6
Subreflector	10	10	3	3	3	15
Total	18	12	7	8	6	25

3.2 Optomechanical Performance

Calculations have been carried out to determine the performance of the antenna proposed. Different models in the finite element programs Ansys and Nastran have been set up. One such model is shown on the cover of this report and in Figure 14. In addition, postprocessors in Matlab have been written.

Table 3. Differential pointing error budget.

Item	Error Type				
	Gravity	Temp.	Wind	Other	Total
Dish	0.1"	0.1"	0.2"		0.23"
Quadruopod	0.1"	0.1"	0.2"	0.1"	0.25"
Elev. struct.		0.1"	0.2"	0.1"	0.24"
Yoke		0.2"	0.2"		0.28"
Base & Az ring		0.1"	0.2"	0.1"	0.24"
Encoder				0.1"	0.10"
Servo			0.2"	0.1"	0.22"
Foundation			0.1"		0.10"
Nulling					0.20"
Total	0.07"	0.28"	0.50"	0.22"	0.65"

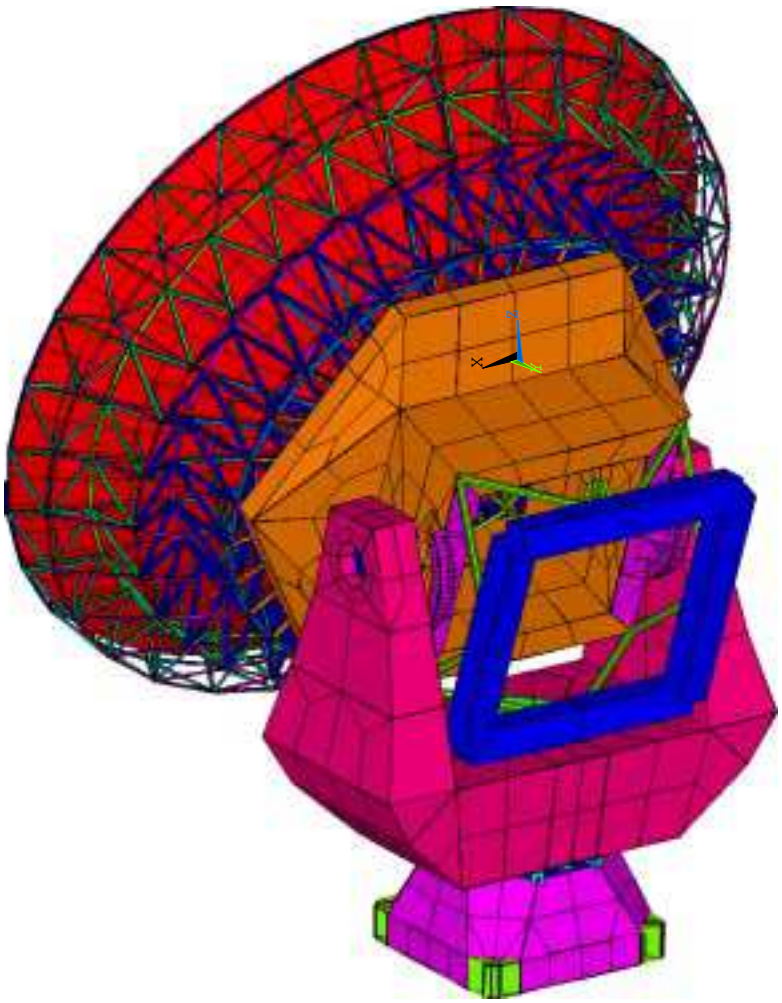

Figure 14. Finite element model of the radio telescope.

3.2.1 Gravity Load

The antenna can be pointed in different directions with respect to gravity. This introduces gravity deflections in the dish and the structure. A rotation in azimuth does not change the direction of the gravity vector with respect to the antenna. Azimuth rotation can therefore be disregarded in this context. However, changes in elevation pointing angle are important for the gravity deflections.

Gravity deflections influence antenna performance in two ways. Firstly, deflections of the dish may degrade the optical performance because the surface form deviates from the ideal one. Secondly, gravity deflections change the pointing angle of the antenna. To a first approximation, pointing errors due to gravity deflections are not dangerous. They can be handled by tabular corrections to the pointing angles combined with a movement of the subreflector. In addition, the severe differential pointing specification given in Appendix A applies to only a small area of the sky at a time and is therefore not critical for the gravity case.

Dish deformations can be subdivided into two contributions. The first part has the shape of a paraboloid. This part is not critical for image quality, provided that the subreflector is always maintained in its optimal location. The second part, describing the deviation of the deflection from a paraboloid, is a direct measure of main reflector quality. In many cases the influence of the spatial wavelength can be neglected and the quality of the main reflector can simply be described by the rms value of the deviations from a paraboloid obtained by a least-squares approximation.

By adjusting the panels perfectly, the gravity influence can be canceled at a selected elevation angle, the rigging angle. For the present design, the rigging angle has been chosen as 50° in elevation. As a consequence of the adjustment, any gravity deflections existing when the telescope is pointing in elevation to the rigging angle, become built into the reflector surface with negative sign. For all other elevation angles, only the deviation in deflections from those at the rigging angle play a role. And, as stated above, only the part of it that does not have the shape of a paraboloid is important.

The performance under gravity load has been studied on the basis of an Ansys finite element model and a Matlab postprocessor. Figure 15 shows an example of such a computation. The results from computations for different elevation angles can be found in Table 4. The antenna can move in elevation in the range 15° to 95°. However, most observations take place in the range 20° to 75° and therefore this range is of main

interest. Assuming that all of these values are of equal astronomical interest (which is a conservative assumption) a weighted average has been computed as shown in the table.

The conclusion is that for the present antenna design, gravity induced surface errors will amount to about 3 μm rms. This is within the error budget.

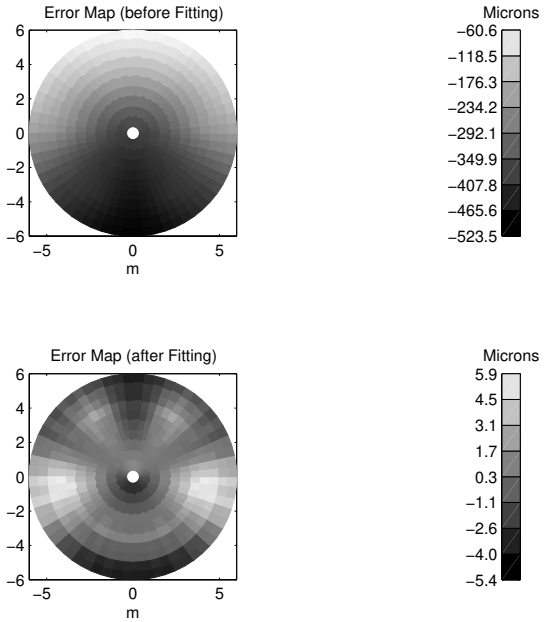

Figure 15. Example of gravity computation based on a finite element model. The elevation angle is 60°. The upper contour plot shows the raw surface deflection (normal to the surface) with respect to a weightless telescope. The lower plot shows the same surface after rigging angle corrections are introduced, and after the paraboloid part has been removed by postprocessing.

Table 4. Gravity induced main reflector surface errors.

Elevation Angle	Surface Errors, μm rms	
	Without rigging angle compensation	With rigging angle compensation
20°	9.3	7.6
35°	12	3.6
50°	14	0
60°	15	2.1
75°	17	5
Weighted Average	13	3.2

3.2.2 Wind Load

Wind forces deform the antenna structure and degrade image quality and pointing precision. Due to the stochastic nature of wind, it is not possible to compensate for wind effects using predetermined tabular corrections as for gravity deflections.

A finite element calculation was carried out to study wind effects. The same finite element model as described in the preceding section has been used. Generally available JPL wind tunnel data were applied since no specific wind tunnel measurements have been carried out for this antenna. For simplicity, it has been assumed that the wind comes directly from the front or the back of the antenna. Hence, for the purpose of these calculations, wind effects are a function of elevation angle only.

The results are presented in Table 5. It is seen that the main reflector surface errors are negligible at this wind speed. The pointing errors are within the total specification of 0.66". On one hand, the present antenna design has not been optimized. Thus some improvement seems possible. On the other hand, effects have not been studied for all pointing angles with respect to wind, and accurate wind load data are not available at this time. The conclusion is that it seems possible to fulfill the pointing specification of 0.66" at 6 m/s wind velocity but the final proof cannot be given before a more thorough study has been carried out.

Table 5. Wind effects for different elevation angles.
Wind comes directly from front or back.

Elevation angle	Main reflector error, μm rms	Pointing error
0°	0.7	-0.40"
60°	2.6	-0.11"
90°	0.4	-0.21"
120°	1.0	0.37"
180°	0.5	0.27"

It is of interest to determine from where in the antenna the pointing errors arise. This can be seen from Table 6. The angular deflection of the fork arm is measured at the elevation bearing where the elevation encoder would be placed. It can be seen that the CFRP BUS, the dish, the subreflector and the receiver to a good approximation deflect in tilt as a rigid body under wind load. The angular deflections essentially arise in the steel structures below elevation axis and between elevation axis and the CFRP BUS. It can also be seen that the angular deflections can be reduced significantly by measuring and compensating for the tilt of the fork arms at the location of the elevation axis. More comments on this option will be given in section 4.

Table 6. Angular deflection at different locations of the structure.

Elevation angle	Angular deflection of fork Arm	Angular deflection below CFRP structure	Angular deflection of antenna surface (best fit)
0°	-0.40"	-0.39"	-0.40"
60	-0.18"	-0.15"	-0.11"
90	-0.10"	-0.15"	-0.21"
120	0.16"	0.23"	0.37"
180	0.27"	0.26"	0.27"

3.2.3 Thermal Load

At this time, no thermal calculations have been performed. This will be a point of high priority in the future. Due to changes in temperature and to temperature gradients, there will be deflections in the lower steel structure, to a limited extent in the CFRP backing structure, and in the aluminum panels.

It is not expected that the thermal performance will exclude use of the proposed telescope in the submillimeter range. Firstly because thermal variations typically are slow and secondly because the dish is made of CFRP with a coefficient of expansion much below that of steel. There are thermal expansion members between the CFRP and the steel structures.

3.2.4 Eigenfrequencies

The magnitude of the lowest eigenfrequency does not directly influence the performance of the telescope. However, the value is important for the definition of the obtainable bandwidth of the main servos and thereby the tracking precision achievable. Also, it is a measure of the stiffness of the structure and thereby of the stability of the telescope with respect to static and dynamic disturbances.

Using the finite element model shown in Figure 14, the lowest eigenfrequency of the proposed antenna has been computed to be 8.5 Hz. The form of the corresponding eigenmode is shown in Figure 16. It is a vibration resembling a nodding movement of the telescope. Appendix B is a reprint of a plot of a large number of measured locked rotor resonance frequencies for existing radio telescopes and communication antennas. It can be seen that, from an empirical point of view, the achieved value for the eigenfrequency is satisfactory. On one hand, the value of the eigenfrequency is only a prediction and the real measured value may be lower. On the other hand, further optimization may lead to a higher value.

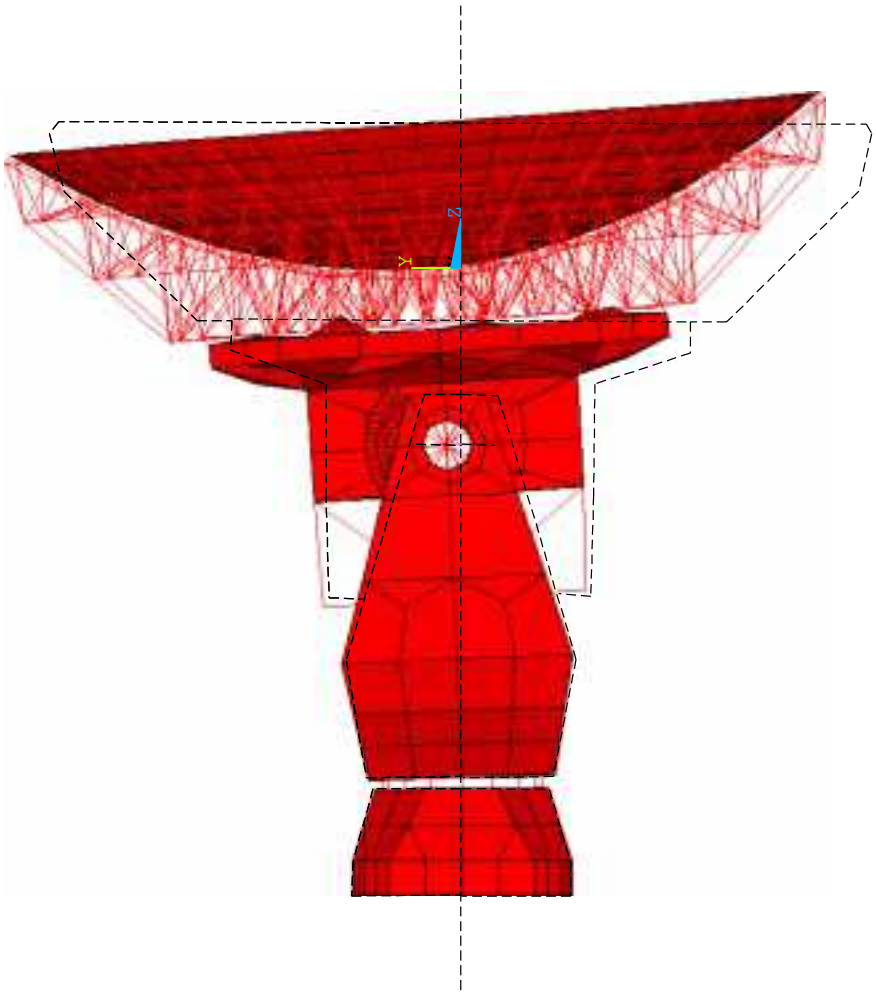

Figure 16. Shape of the eigenmode corresponding to the lowest eigenfrequency.

4. Prospects of Active Optics

4.1 Active Optics

Active optics corrects for telescope errors. It is a computer controlled closed-loop system that analyzes the image and corrects shapes and positions of optical elements to improve image quality. Active optics is now finding widespread use in optical telescopes to correct for slow errors, such as those caused by gravity and thermal effects. The bandwidth of a system is typically of the order of 0.02 Hz.

Active optics is of interest for submillimeter radio telescopes to correct for thermal effects and gravity effects. However, for submillimeter telescopes, wind normally has a significant influence on telescope performance. It is therefore essential for such telescopes that an active optics system can also correct for wind effects. This requires that such a system has a bandwidth that is higher than for optical telescopes. It must be somewhat higher than the lowest structural resonance frequency of the telescope, i.e. 10-15 Hz.

Until now, active optics has not been used for millimeter and submillimeter telescopes. It has been technically difficult to construct suitable metrology systems. One must rely upon internal metrology systems to determine form and position of the optical elements.

4.2 Active Optics on Radio Telescopes

Active optics on radio telescopes can be conceived at different levels:

- *Pointing correction*. By means of an internal metrology system (for instance based on laser measurements), pointing errors are corrected via the azimuth and elevation drives. Such a system can relatively easily compensate for structural deflections in the structure below the antenna dish. Pointing errors caused by deflections of the dish are more difficult to handle.

- *Low spatial frequency correction*. By means of a laser system, aberrations of low spatial order are measured and proper corrections are introduced by actuators. Figure 17 shows a possible implementation of such an internal metrology system. Figure 18 shows how astigmatism in one direction can be corrected with a single actuator placed behind the subreflector.

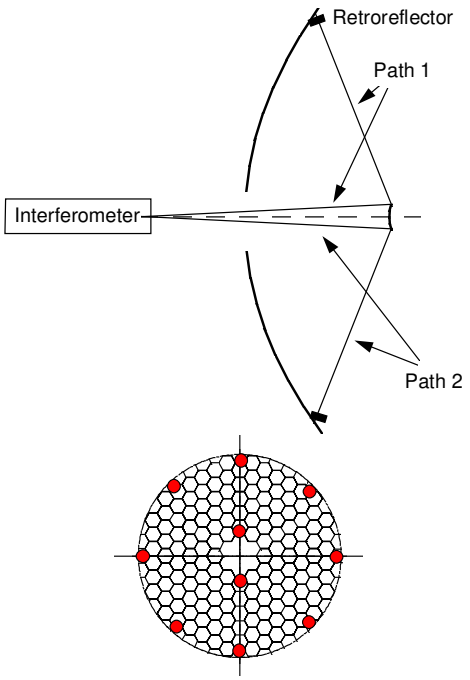

Figure 17. Possible implementation of active optics for low spatial frequency corrections. The upper drawing shows possible laser paths. The lower sketch (here shown with hexagonal panels) illustrates that the form of the antenna dish is measured only at a few carefully selected points. This system could correct for changes in focus, astigmatism, triangular coma and quadratic astigmatism.

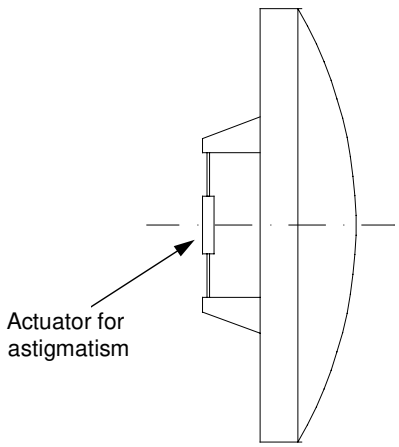

Figure 18. Correction for astigmatism using a single actuator behind the subreflector.

- *Full image correction*. A full image correction would require actuators at all support points of the panels.

4.3 Actions Proposed

As shown in section 3, all calculations indicate that the proposed 12 m antenna will fulfill specifications. On the other hand, the safety margin is not overwhelming. In addition, more detailed calculations are still needed for verification. Hence, as a safety precaution it seems attractive to develop a laser system that corrects for deflections in the steel structures below the elevation axis. Figure 19 shows one possible layout of such a system. It may well be that use of such a system would make it feasible to construct submillimeter telescopes of this type with dishes above 12 m.

The system in Figure 19 has an optical bench located inside the fork and resting on three points near the azimuth bearing. The bench is not loaded by external forces and does not change form during antenna use. It has a double laser system that sends light out to the sides. The light is bent 90° by mirrors or pentaprisms and goes up inside each of the two fork arms. In the top of the fork arms, near the elevation bearings, there are reflective targets. In addition to these systems, laser light is sent down to the foundation where there is a horizontal reflective target. One solution would be to implement this target as a free Mercury surface but there are also other ways of establishing a horizontal target.

The system measures tilt at the location of the elevation axis with respect to the horizontal plane. This is done by using twin laser beams in each arm. They intercept the reflective targets at a small distance from each other. By comparing the returned beams in a Michelson type interferometer, tilt can be readily determined. If needed, the laser beams could run inside tubes that are evacuated or simply thermally insulated. It would also be possible to measure arm deflections but a careful study is needed to determine if this is required.

A system as outlined to measure tilt with a resolution of 0.01" is already in use in optical telescopes today. It is expected that such a system can be series produced at a reasonable cost (200 kDEM?) and with high reliability.

For the purpose of initial alignment, internal surface metrology systems would be highly attractive. In addition, such systems could at a later stage be highly useful for active optics to provide on-line corrections of image quality. Even without active optics, it would be of interest to install such systems permanently on the telescopes, since it would permit a frequent check of the surface quality of the many antennas of the array. Consequently, to reduce project vulnerability it would be prudent to initiate a study of robust antenna surface metrology systems.

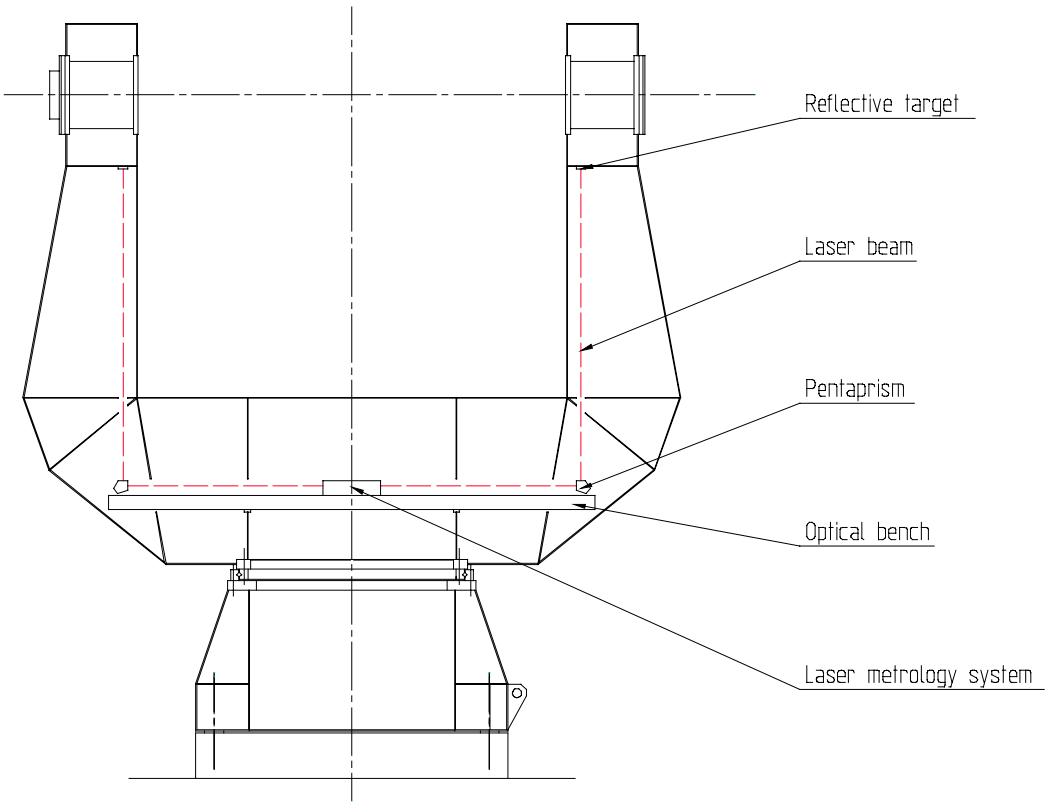

Figure 19. A possible layout of a simple active optics system for pointing corrections. Structural deformations below elevation axis are measured.

In conclusion it is therefore proposed to

- develop laser based systems for pointing correction and install such systems on all antennas,
- initiate studies of a laser based systems to measure the antenna reflector surface on-line. It should be decided at a later moment whether such systems should be installed on the telescope or be applied for initial alignment.

5. Antenna Handling

It has not been the intention to carry out a more detailed study of the telescope operation at this time. However, two operational aspects are important to the design and have therefore been looked into. The first of these is related to configuration changes, i.e. transport of telescopes between the different observing stations. The second one is concerned with the assembly and maintenance halls that will be required. Both of these are dealt with in the following.

5.1 Transporter

The telescopes must be transported between the various observing stations. Truck transport seems to be the most economical solution. The telescopes have a total mass of about 50 tons and the transport must take place on dirt roads in the desert. Hence a dedicated truck (a *transporter*) will be needed. One possible design of a transporter is shown in Figure 20.

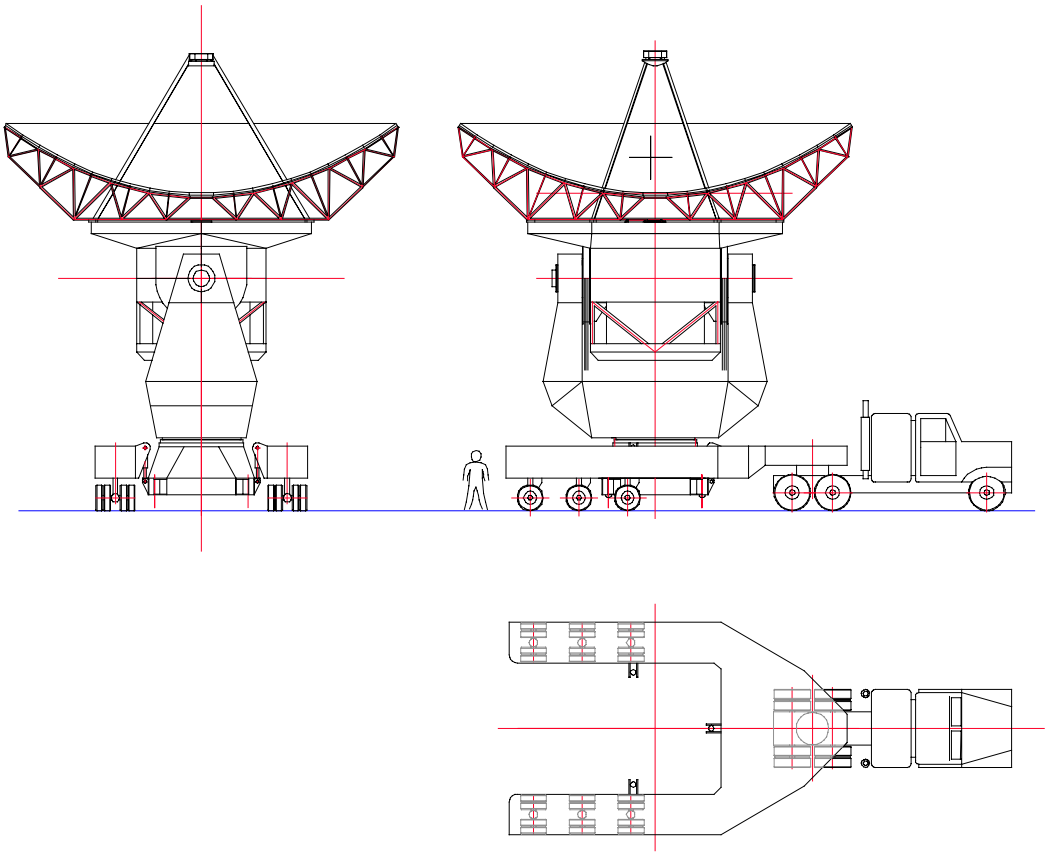

Figure 20. A possible transporter design.

The transporter has an U-shape and fits around the antenna foundation and base. It has eight axles to distribute the load appropriately. The wheel units are of a commercially available type with hydraulic suspension and hydraulic control. A part of the vertical load is carried by a conventional truck, thereby assuring proper road contact for decelerations and accelerations.

The transporter picks up the antenna by means of three free hanging hydraulic cylinders. The cylinders can be attached manually to fixation brackets on the side of the antenna base. Hydraulic control of the cylinders allows both a parallel up/down movement and a leveling movement of the antenna. Use of free hanging cylinders has the advantage of giving lateral freedom when the antenna is picked up or lowered down onto a foundation. This freedom is required because the transporter cannot be backed up to the antenna with high precision.

It has been verified that the transporter with the antenna can be inclined by 10% and braked with 0.3 g simultaneously. The influence of wind and earthquakes must be studied. Obviously, there will be an upper limit for the wind speed at which a movement of an antenna with the transporter is allowed.

For reasons of reliability, it is necessary to have at least two transporters. To provide a quick configuration change, it may be desirable to build 3-4 of these.

5.2 Assembly and Maintenance Halls

For reasons of efficiency, it is important to assemble the telescopes at a low altitude. This can best be done in a facility in (or near) San Pedro d'Atacama. Therefore an assembly hall at this location is needed. Transport from San Pedro to the Chajnantor site can be done with one of the transporters.

For maintenance purposes, an antenna hall is required on the site. The hall should be large enough to hold one antenna pointing in any direction. The antennas can be transported to the hall using the transporter.

6. Project Execution

6.1 Project Execution Principles

Due to the large number of antennas that must be manufactured, it will be attractive to manufacture two or three prototypes. The first prototype will be used to check that the design is adequate and that the specifications can be fulfilled. The second prototype should be further developed so that it is optimal from a production point of view. It is a series production prototype. These two prototypes should remain on a test site close to one of the participating institutes. They could serve as a test bed for future developments. The third and final prototype is the first antenna of the series production. To train assembly personnel this antenna should be assembled at a manufacturing plant in one of the member countries or at the test site referred to above. It should also be tested as a complete unit by observatory staff. After testing, the antenna can be dismantled and transported to the final site.

It is foreseen that the antennas are transported to the assembly site near San Pedro subdivided into the largest subassemblies possible. There will be the following subassemblies: Base with large ring bearing and motor, fork with elevation bearings and motors, center section with receiver cabin and dish interface steel structure, BUS of CFRP, panels, quadrupod, and subreflector unit. The BUS will be a large but light unit and can possibly be transported by helicopter form Antofagosta to San Pedro. It is not recommended to transport the complete telescope by sea as one unit, since the highly precise bearings may be damaged during transport due to vibrations. Transport from San Pedro to Chajnantor should be done by means of the antenna transporters.

An antenna development and fabrication project can be executed in different ways. Which way that is optimal depends to a large extent on the funding environment and the organizational structure of the institution supervising execution. Two typical execution scenarios can be outlined.

- In-house Development
  The antennas are designed by a project group established for the purpose by the executing institution. Following the development and design phase, manufacture is given to different companies, each with different specialties. Assembly of the prototypes is done under the responsibility of the project group. The development, design and system responsibility lies with the executing institution.

- Design by Contractor

A predesign is carried out by a project group of the executing institution. Thereafter a contract for the overall design is given to two or three competing teams. Subsequently a selection among these (or a combination) is done and a contract is given to a company to design and fabricate two prototypes along these lines. The first prototype is used to verify the design principles and the second one to check series production aspects. Thereafter a contract for manufacture of all antennas according to drawings is placed. Alternatively (in fact preferable), the antennas may be subdivided into two lots that are produced in parallel by different two different contractors. This reduces project vulnerability to supplier instability and yet gives the full advantages of mass production. Assembly in Chile may be done under the responsibility of the executing institution.

The first approach is more cost-effective but the risks involved are somewhat higher than for the second one. The second one also has the advantage of spreading the development know-how in the member countries.

6.2 Time Schedule

A time schedule for the antenna project is shown in the diagram below. The schedule indicates the shortest possible execution time with the budget presented in section 6.3. This time schedule is based purely on engineering considerations. There may be reasons to construct the telescopes slower. Erection is assumed to take place in parallel with fabrication of the telescopes.

Task	**1998**				**1999**				**2000**				**2001**				**2002**				**2003**			
	1	**2**	**3**	**4**	**1**	**2**	**3**	**4**	**1**	**2**	**3**	**4**	**1**	**2**	**3**	**4**	**1**	**2**	**3**	**4**	**1**	**2**	**3**	**4**
Project group studies	X	X																						
Studies by 2-3 contractors			X	X																				
Final design						X	X																	
Fabrication and test of prototypes									X	X	X	X												
Manufacture and erection of antennas													X	X	X	X	X	X	X	X	X	X	X	X
Development of pointing correction system			X	X	X	X	X	X																
Fabrication of pointing correction systems									X				X	X	X	X	X	X						
Studies of surface measuring systems			X	X	X	X	X	X	X	X	X	X												

6.3 Budget

A tentative budget for fabrication of an antenna is shown on the following page. The cost is a unit price for one antenna produced by series fabrication. In addition, for each antenna, four different foundations are included. Site erection is not included in this budget.

The budget has been set up in German Marks (DEM). For convenience, a conversion to US-Dollars (USD) is shown. An exchange rate of 1.800 between the two currencies has been applied. This conversion factor was valid on September 23, 1997.

Table 7. Tentative budget for one antenna and four foundations. Computer control systems is not included but power amplifiers are.

Component	**Cost basis**	**Cost** ($kDEM_{97}$)	**Cost** ($kUSD_{97}$)
Reflector:			
Panels	390 DEM/kg	753	423
Panel adjusters	100 DEM/kg	20	11
Deicing system	None	0	0
CFRP BUS	400 DEM/kg	900	506
BUS temp control	None	0	0
Elevation struct.+cntrwgt	8 DEM/kg	153	86
Quadrupod and M2-unit		68	38
Apex mechanism	50 DEM/kg	4	2
Subreflector	390 DEM/kg	10	6
BUS insulation	None	0	0
Cabin details	Estimate	5	3
Reflector assembly	None	0	0
Subtotal		1913	1075
Mount:			
Base & yoke	10 DEM/kg +...	269	151
Bearings	Supplier info	62	35
Encoders	Supplier info	60	34
Motors and amplifiers	Supplier info	98	55
Active mount metrology	Tentative	200	112
Cabling & cable wraps		40	22
Mount assembly	320 hours	32	18
Four foundations	600 DEM/m^3 incl. all	31	17
Four cups in concrete	Four cups	8	4
Subtotal		800	450
Management, etc:			
Shipping to MMA site	200 DEM/m^3	157	88
Overhead, etc: 30%		1531	860
Contingency 15%		660	371
Subtotal		1688	1319
Total		5061	2844

7. Conclusions

A predesign for a 12 m telescope with a Carbon Fibre Reinforced Plastic dish structure has been presented. Calculations have shown that the telescope will fulfill requirements for a submillimeter telescope. However, it should be noted that only calculations for representative cases have been carried out. A more detailed study will be needed to deliver the final proof that an antenna as proposed will fulfill all specifications

A differential pointing precision of 0.66" rms is required. This seems to be the most critical of all specifications. Representative computations indicate that wind disturbances will cause pointing errors below 0.4" rms. Although there are also other error sources, this seems acceptable. More detailed computations are required for a full verification since the calculation of wind sensitivity has been based only on representative cases.

To provide a larger safety margin, or alternatively a larger dish, it is attractive to develop a simple active optics system to correct for pointing errors caused by deflections in the steel structure below the elevation axis for frequencies up to 10-15 Hz. A possible implementation scheme has been presented.

The specification of 25 μm rms for the surface precision can be fulfilled. The initial alignment precision of the panels is of importance. For this and other reasons, study of a robust on-line surface measuring system should be initiated to reduce project vulnerability.

8. Appendix A: Specifications

Array

Site	Chajnantor, Chile	
Altitude	5025 m	
Antennas	60	Tentative
Foundations	240	Tentative
Configurations No of configurations No of different configurations per year	 5 3	 Typ. Typ.
Distance between antennas	1.286∗D = 15.430 m	Min.
Antenna move	0.5 h 0.5 h 10 km/h	Picking up Setting down Transport velocity

Antenna System

Pointing and Tracking: Azimuth Elevation Blind pointing Differential pointing (<½ h, <10° offset) Tracking Switching between adjacent objects	 ± 270° 15°-95° 20°-75° <5" rms <1/30 BW at 300 GHz (0.66") rms 0.2" rms 1.5 sec /1.5°	 Full range Typical observing range Target value See chapter 3
Slewing velocity	4°/s	
Phase stability	<10 μm rms	For frequencies > 1Hz and wind velocity < 6 m/s
Observations of Sun	Allowed	

Wind: Full specification range Reduced specifications	 v < 6 m/s 6 m/s < v <15 m/s	 Mean speed 10 m above ground
Nutating subreflector	None	
Survival Wind Earthquake	 60 m/s 7 Richter[1] 8.5 Richter[1]	 Mean, 10 m height Insignificant damage Repairable within 3 weeks

[1] Spectrum TBD

Optics

Configuration	Cassegrain	
Main reflector: F-ratio Radius of curvature Eccentricity Focal length Ext. diameter Int. diameter	 f/0.35 8.4 m 1 4.2 m 12 m 0.77 m	 Appr.
Subreflector: Radius of curvature Eccentricity Focal length Diameter	 0.562 1.092 0.56 m 0.77 m	 Appr.
Exit f-ratio	f/8	
Scale	0.465 mm/"	
Beam width 3dB	17.4" 19.8"	Without tapering With 10 dB tapering
Shaping	None	

Mechanics

Mount	Alt/az	
Receiver cabin	3 m ∗ 3 m ∗3.75 m	Appr.
Rigging angle	50°	

Panels		
No	135	
Material	Ligthweighted Al	
No of supports per panel	5	
Surface Protection		
Steel	Painting	
Panels	Aludine	
Mass, total	Appr. 50 t	
Panels	2 t	
Back Up Structure (BUS)	2.3 t	
Center section	9.8 t	
Counterweight	9.7 t	
Fork	17 t	
Base	8.9 t	
Total	50 t	

9. Appendix B: Locked Rotor Resonance Frequencies